Chin. J. Astron. Astrophys. Vol. 6 (2006), No. 5, 608–616
(*http://www.chjaa.org*)

Chinese Journal of
Astronomy and
Astrophysics

An Impulsive Heating Model for the Evolution of Coronal Loops *

Li Feng[1,2] and Wei-Qun Gan[1]

[1] Purple Mountain Observatory, Chinese Academy of Sciences, Nanjing 210008; *lfeng@pmo.ac.cn*
[2] Max Planck Institute for Solar System Research, Max-Planck-Str. 2, 37191, Katlenburg-Lindau, Germany

Received 2006 February 8; accepted 2006 March 9

Abstract It was suggested by Parker that the solar corona is heated by many small energy release events generally called microflares or nanoflares. More and more observations showed flows and intensity variations in nonflaring loops. Both theories and observations have indicated that the heating of coronal loops should actually be unsteady. Using SOLFTM (Solar Flux Tube Model), we investigate the hydrodynamics of coronal loops undergoing different manners of impulsive heating with the same total energy deposition. The half length of the loops is 110 Mm, a typical length of active region loops. We divide the loops into two categories: loops that experience catastrophic cooling and loops that do not. It is found that when the nanoflare heating sources are in the coronal part, the loops are in non-catastrophic-cooling state and their evolutions are similar. When the heating is localized below the transition region, the loops evolve in quite different ways. It is shown that with increasing number of heating pulses and inter-pulse time, the catastrophic cooling is weakened, delayed, or even disappears altogether.

Key words: hydrodynamics — Sun: corona — Sun: transition region

1 INTRODUCTION

The nature of the coronal energy source remains one of the most significant unsolved problems in solar and stellar physics, though it is recognized that magnetic field plays an important role in it. EUV and X-ray observations showed that coronal loops that outline the coronal magnetic field are the dominant structures in the outer solar atmosphere. Recently there has been great interest in the idea that the corona is heated by numerous small energy release events called "nanoflares" (Parker 1988). These events are probably due to localized magnetic reconnections formed by slow motion of the photospheric footpoints.

Winebarger et al. (2003) compared 67 loops observed by TRACE or SXT with steady heating models and found that only 19 are fully consistent with hydrodynamic solutions of steady heating. Impulsive heating models are therefore needed to explain the observations. Reale et al. (1994) made some hydrodynamic calculations for a loop heated by a random sequence of pulses localized at the loop apex. Their synthesized results indicated that variable heating may be the cause of variability in some SXT loops, but for the EIT loop, the heating might make some parts of the loop keep on appearing and disappearing while its base remains quite bright. Betta et al. (1999) also modelled the hydrodynamics of coronal loops that are subjected to a random energy deposition around the loop top and synthesized some emission lines formed in the transition region. The results were qualitatively consistent with SUMER observations; quantitatively, they were slightly different.

High resolution observations like SOHO and TRACE have revealed a type of very small scale activity at transition region temperatures. Due to their high frequency of occurrence, they could be one of the heating

* Supported by the National Natural Science Foundation of China.

sources of the solar corona. Mendoza-Briceño et al. (2002) have investigated the response of a small loop of 10 Mm to microscale heating pulses periodically and randomly injected below the transition region. It is found that such successive energy inputs can maintain the plasma in the loop at typical coronal temperatures and the temperature distribution derived is in good qualitative agreement with TRACE observations of isothermal loops (Aschwanden et al. 2001a). An investigation on the elapsed time between successive pulses showed that increasing the elapsed time would decrease the overall loop temperature and when a critical value is reached, the loop would undergo catastrophic cooling (Mendoza-Briceño & Erdélyi 2004).

Where the heating occurs is still controversial among the researchers. Even for the same loop observed by SXT, different authors derived quite different conclusions(Priest et al. 2000; Aschwanden 2001b; Reale et al. 2002). It is important to follow the temporal evolutions of active region loops with heating at different positions. Testa et al. (2005) has found that the spatial extent of the heating is a fundamental parameter for determining whether or not the loop would experience a catastrophic cooling. In the frame of nanoflare heating, energy is released in some localized regions. For a loop heated by just one pulse, there will also be a critical value of the heating position that will decide whether or not the loop will collapse. One of the goals of this paper is to identify the conditions under which loops subject to different manners of nanoflare heating will have similar or different properties. Another goal is to track the evolution of a loop with different temporal profiles of this kind of heating.

2 HYDRODYNAMIC MODEL

Because the plasma parameter β is much smaller than unity in the solar corona, the plasma is dominated by the magnetic field. We assume a semicircular flux tube with a constant cross section in which all physical quantities vary only along the field lines. To solve the hydrodynamic loop equations we apply the NRL Solar Flux Tube Model (SOLFTM). The basic parameters and assumptions are the same as in the previous simulations with this code (Mariska 1987; Mariska et al. 1989). For more details about this numerical model, one can refer to the RHESSI version of SOLFTM given in the homepage of Mariska. We adopt the same heating function as did Warren et al. (2003) and Winebarger & Warren (2004),

$$E_H(s,t) = E_0 + g(t)E_F \exp[-(s-s_0)^2/2\sigma_s^2], \tag{1}$$

where s_0 designates the central location of the impulsive heating, σ_s is the spatial width of the heating, and E_F is a constant that determines the maximum amplitude of the heating. The gaussian function is adopted here to mimic the nanoflare heating. The function $g(t)$ is chosen to be a simple triangular pulse,

$$g(t) = \begin{cases} t/\delta, & t_0 < t \le t_0 + \delta \\ (2\delta - t)/\delta, & t_0 + \delta < t \le t_0 + 2\delta \end{cases} \tag{2}$$

where t_0 is the beginning time of the pulse and 2δ is the duration of the pulse. The term E_0 is always present, and the loop will eventually return to equilibrium.

For the simulations that will be made in this paper we choose the loop half length of 110 Mm as did Winebarger & Warren (2004). It is the length of typical active region loops. The background volumetric heating rate is assumed to be 1.5×10^{-6} erg cm^{-3} s^{-1}. This value can be obtained from the RTV scaling laws (Rosner et al. 1978) which describe the relationship among the maximum temperature, base pressure and uniform heating rate in the loop. In the simulations the loop is assumed to be heated symmetrically, and only the evolution of one half of the loop needs to be calculated. The initial conditions are shown in Figure 1 with velocity equal to zero at $t = 0$. The maximum temperature at the loop top is about 1 MK, and the density is too low to be observed by any instruments from EUV to soft X-ray wavelength.

The numerical grid for most of the simulations consists of 2400 elements distributed over three regions. A chromospheric region is initially 1.0×10^9 cm deep and has 800 elements with exponentially increasing spatial spacing. The next 400 elements have a constant spacing of 4×10^5 cm and cover the upper chromosphere, the transition region and the lower corona. The remaining 1200 elements cover the remainder of the corona with exponentially decreasing spatial spacing. Moreover, sometimes we will increase the number of grids when the code fails to converge.

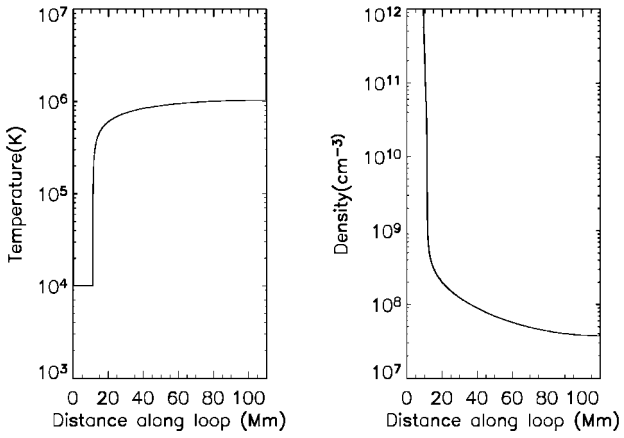

Fig. 1 Initial atmosphere of the coronal loop: temperature and electron density distributions along the loop.

3 NUMERICAL RESULTS

To simulate the nanoflare heating released in the loop, we have chosen the maximum amplitude of the heating $E_F = 1$ erg cm^{-3} s^{-1}, and the spatial width of the heating $\sigma_s = 6 \times 10^7$ cm. Total heating deposition into the loop is 10^{27} erg. In all of the simulations in Sections 3.1 and 3.2 these three parameters are the same. To follow the coronal response of the loop to the heating, we analyze the averaged values from 30 Mm to the loop top. Note that the exact choice of this lower boundary does not significantly influence the results and could be set to any position well above the transition region.

3.1 Loop Evolution for One Single Pulse

The evolution of the loop is usually exhibited in the density-temperature diagram. Winebarger & Warren (2004) have discussed the evolution of a coronal loop subjected to an impulsive heating with different parameters. The apex density is plotted as a function of the apex temperature. They found that once the impulsive heating is turned off, the loop begins to cool by conductive loss. At the end of the conductive cooling phase, the evolution passes through an equilibrium point, at which the conductive and radiative cooling times are equal. After this point, the loop mainly cools by radiative loss until it eventually returns to its initial atmosphere (see their fig. 1 for detail). Through a set of simulations they found that typical TRACE observations of cooling loops do not provide adequate information to discriminate the magnitude, duration, or location of the energy deposition.

We have made some similar simulations and obtained similar results. Figure 2 shows the density-temperature plots with the energy release at 25 Mm and 50 Mm, two different positions in the coronal part of the loop. All the energy is released in a single pulse of 500 s. The solid beeline is derived by setting the conductive and radiative cooling time scales equal. As shown by Winebarger & Warren (2004), the solutions are different only in the initial heating and conductive cooling phase of the loop evolution. Comparing the asterisk in each line, we find that during the initial heating phase, the solution with the lower heating position has a lower temperature and a higher density. It is difficult for a given heating at the lower position to increase the temperature. Furthermore, the initial higher density for $s_0 = 25$ Mm is mainly due to the steeper temperature gradient that develops around the transition region which will lead to a stronger chromosphere evaporation.

However, if the energy release is in an even lower layer, say, the top of the chromosphere, then the loop will evolve quite greatly. Figure 2 shows, for heating sources in the coronal region and below the transition region, there are differences not only in the initial heating and conduction phases but also in the radiative cooling phase. In the case of a lower source of energy release at $s_0 = 10$ Mm, the loop will experience a

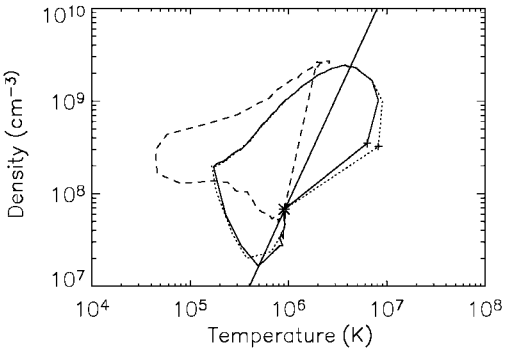

Fig. 2 Averaged density as a function of averaged temperature for three hydrodynamic simulations. Solid line, heating position centered at $s_0 = 25$ Mm; dotted line, $s_0 = 50$ Mm; dashed line, $s_0 = 10$ Mm. The asterisk marks the time when the loop is in its initial equilibrium condition, and the two plus signs mark the time 200 s (in all the density-temperature diagrams of this paper the points are recorded every 200 s and the loops evolve in the counterclockwise direction).

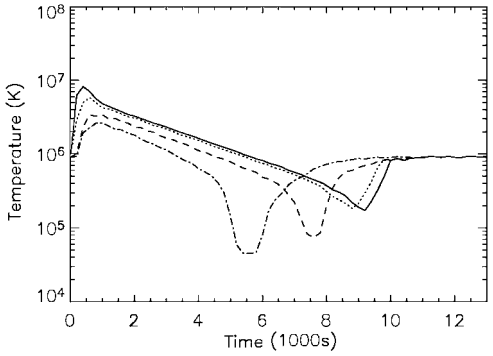

Fig. 3 Time evolution of loop with the heating released at four different positions. Solid line, $s_0 = 25$ Mm, heating in the corona; dotted line, $s_0 = 11.6$ Mm, heating at the base of the corona; dashed line, $s_0 = 10.3$ Mm, heating in the transition region; and dash-dotted line, $s_0 = 10$ Mm, heating at the top of chromosphere.

catastrophic cooling (Schrijver 2001; Müller et al. 2004). The large densities below the transition region cause the energy deposited in the loop to be radiated away so resulting in a very low temperature in the coronal part. Moreover, the low temperature in the upper part will lead to high radiative loss there. Thermal equilibrium at the loop top is gradually broken and the loop rapidly cools down to the transition region temperature and below (less than 0.1 MK).

We make a set of simulations with different heating positions (Fig. 3). The time for the temperature to reach its minimum is earlier by about 500 s when the energy heating is at the base of corona than at the corona itself, while for heating in the transition region, an obvious rapid cooling develops. As we gradually lower the heating position from the coronal part to the chromosphere top in the four case, the loop gradually loses thermal equilibrium and begins to experience a catastrophic cooling. We find the critical value is located in the transition region but is not unique for a given loop as it depends on the heating function and the initial conditions adopted.

3.2 Effects of Different Manners of Nanoflare Heating

In this subsection we follow the evolution of the loop heated by different numbers of pulses and at different times in between: we wish to find out whether, or how these two parameters change the properties of the loop. To vary the number of pulses, we divide a single pulse into five pulses and ten pulses so that each pulse will last either 100 s or 50 s. We vary the elapsed time of the five pulses from 0 s to 300 s.

3.2.1 Results of non-catastrophic-cooling loops

Loops that do not experience catastrophic-cooling are often long-lived during the observations. To study their evolutions, we choose, as example, the loop with the heating centered at $s_0 = 25$ Mm . Figure 4 shows the temperature evolution during the initial 1000 s. We can see that the number of temperature peaks varies with the number of pulses and the maximum temperature decreases with increasing number of pulses. The whole evolutionary cycles of the thee cases of one, five and ten pulses are shown in Figure 5. There is no obvious difference between them after the evolution passed through the equilibrium point. During the heating phase, the loops with multiple pulses get a lower maximum temperature at $t = 400$ s and a higher density at $t = 200$ s. Relative to the single pulse case, the first pulse in the multiple pulse case causes the loop to have a higher temperature and the higher temperature gradient developed above the chromosphere then leads to a larger conductive loss and a stronger chromosphere evaporation.

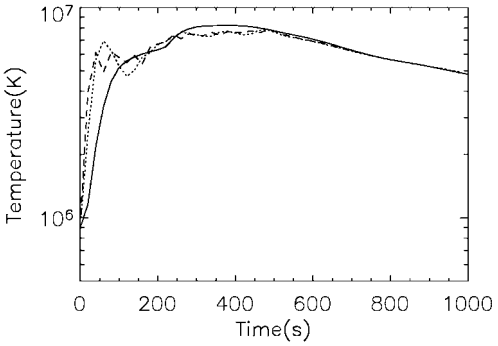

Fig. 4 Averaged temperature as a function of time during the initial 1000 s with the heating located at s_0 = 25 Mm. Solid line, one pulse injected; dotted line, five pulses injected; and dashed line, ten pulses injected.

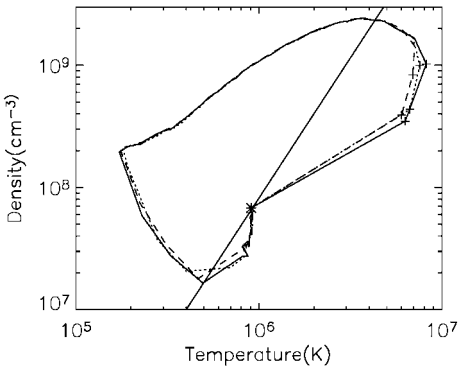

Fig. 5 Averaged density as a function of averaged temperature. Heating position is localized at $s_0 = 25$ Mm. Solid line, one pulse injected; dotted line, five pulses injected; and dashed line, ten pulses injected. The first group of three plus signs mark the time $t = 200$ s, the second group of three plus signs correspond to $t = 400$ s.

Physically, nanoflares may not be consecutively injected, so we set a parameter of elapsed time between successive energy inputs. Figure 6 shows the evolution loops subjected to five pulses with elapsed times 0 s and 300 s. The role of this parameter in the evolution only shows up during the initial 2000 s in the density-temperature diagram. However, in the time evolutions of temperature and density (the middle and bottom panels), differences exist until the loop recovers equilibrium. For the whole evolution cycle, the loops of different elapsed times have similar properties and increasing this parameter just delays the course of evolution. Another obvious effect of the elapsed time is a decrease in the maximum temperature, which is again due to a larger conductive loss to the chromosphere, and more rapid evaporation developed there. The maximum density is almost the same.

From the discussion above, we see that for non-catastrophic-cooling loops, the evolution cycles are similar in the two different manners of nanoflare heating, the results depend weakly on the temporal profile of the heating. Combined with the result of Winebarger & Warren (2004), for the long-lived loops, the evolutions are not sensitive to the heating details, whether done in one relatively large magnetic reconnection event or in multiple small reconnection events like nanoflares.

3.2.2 Results of catastrophic-cooling loops

For catastrophic-cooling loops, we choose the loop subjected to a single pulse with $s_0 = 10$ Mm as reference case in the analysis below.

Unlike the case of non-catastrophic-cooling loops, in the catastrophe cooling case the number of pulses does make a difference on the evolution not only in the initial heating and conductive cooling phases but also in the radiative cooling phase, the differences between a single pulse and multiple pulses being particularly apparent (Fig. 7). This result is in contrast to the conclusion of Winebarger & Warren (2004). From the temperature evolution, we can see that along with increasing number of pulses, the catastrophic cooling gets weaker and more delayed. For a single pulse, it takes about 2000 s for the averaged temperature to decrease from 1 MK to 0.1 MK , while for five pulses this decrease takes 3800 s. Furthermore, the minimum temperature of about 0.1 MK is much higher in multiple than single pulse.

When the elapsed time changes from 0 s to 300 s, the catastrophic cooling almost disappears and a sudden decrease of temperature appears in the initial few hundred seconds (Fig. 8). After the earlier pulse ceases, the temperature would decrease, then the radiative cooling would be enhanced. If the next pulse is not injected in time, thermal equilibrium will be broken and then a rapid cooling will develop.

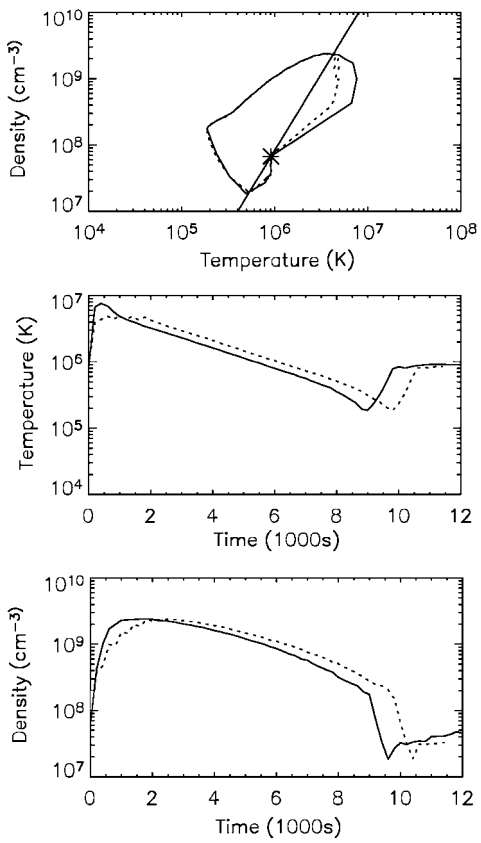

Fig. 6 Top: averaged density as a function of averaged temperature. Middle and bottom: averaged temperature and density as functions of time. Heating is localized at $s_0 = 25$ Mm. Solid line, elapsed time 0 s; dotted line, elapsed time 300 s.

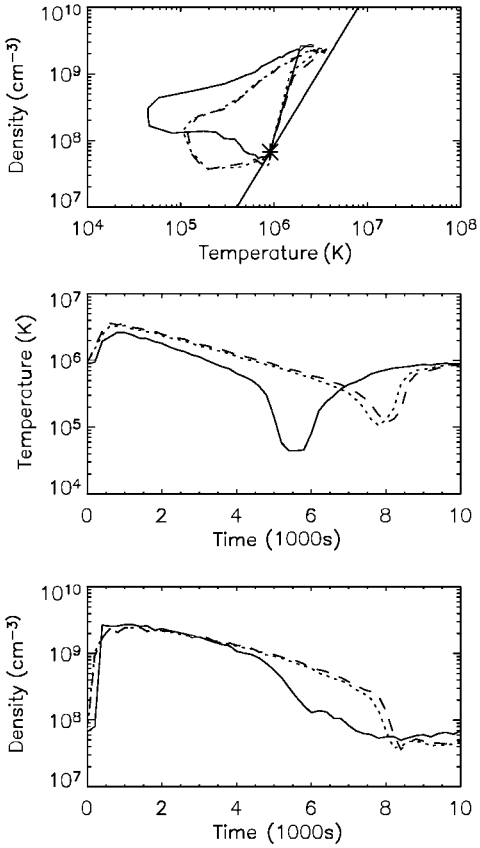

Fig. 7 Top: averaged density as a function of averaged temperature. Middle and bottom: averaged temperature and density as functions of time. Heating is localized at $s_0 = 10$ Mm. Solid line, one pulse injected; dotted line, five pulses injected; dashed line, ten pulses injected.

We can see from above that, when the heating is below the transition region, the loop evolution is sensitive to the details of the nanoflare heating. Increasing the number of pulses and the elapsed time in between can weaken the catastrophic cooling or even make it disappear. In other words, the more concentrated in time the heating is, the more likely catastrophic cooling will happen. We have checked with calculations in three cases of one single pulse, of five consecutive pulses and of five pulses with 300 s between the successive pulses. Figure 9 shows, as the number of pulses or the time in between increases, there is increasing evidence a plasma downflow from the top of the loop (at 85 Mm to 110 Mm) to its lower portions. The downflow near the top will decrease the density there, and hence decrease the radiative loss: the stronger the downflow, the lower the radiative loss. That is why we find that the catastrophic cooling is weakened and even disappears altogether.

4 DISCUSSION AND CONCLUSIONS

Recently there has been some work concerning the availability of TRACE diagnosis to the details of the heating. Our results show if the loop is long-lived, then it is hard for TRACE to distinguish among different heating parameters. This is consistent with the conclusion of Winebarger & Warren (2004), which they arrived at through a set of simulations of heating by a single pulse. It has been indicated that for this kind

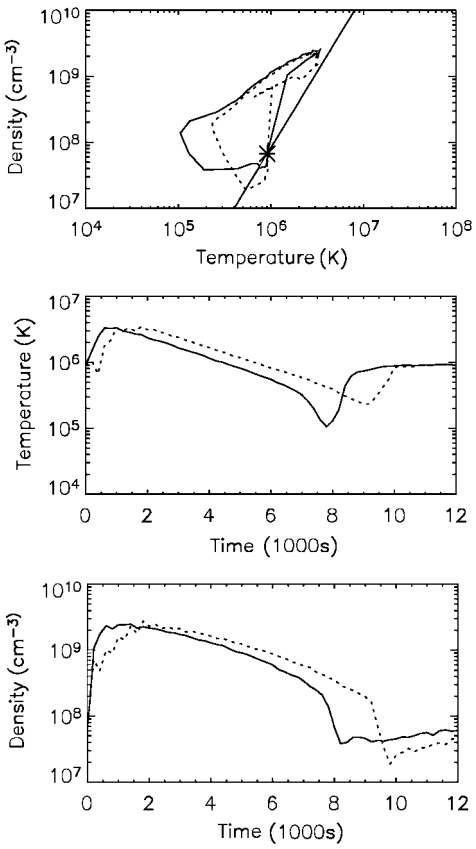

Fig. 8 Top: averaged density as a function of averaged temperature. Middle and bottom: averaged temperature and density as functions of time. Heating is localized at $s_0 = 10$ Mm. Solid line, elapsed time equals 0 s; dotted line, elapsed time is 300 s.

of loops the evolution is not sensitive to the heating details, whether they are heated by one relatively large magnetic reconnection event or by multiple small reconnection events like nanoflares.

On the other hand, for the catastrophic-cooling loops, the evolution differs greatly and the differences can be shown in the TRACE observations. We have calculated the intensity evolution in TRACE 171 Å filter for Figure 7. The intensities are calculated using TRACE_T_RESP in the solar software and the width along the line of sight is assumed to be 3 Mm. From Figure 10 we can see that the loop evolutions in the TRACE observation are quite different. Different evolutions can also be derived from figure 1 of Mendoza-Brice ñoet al. (2005) for the catastrophic-cooling cases. The short loops in their paper are heated by 10 random pulses near the footpoints. For the first loop, there is obvious difference in the temperature evolution between elapsed times 220 s and 240 s.

The response of the loop becomes more sensitive to the details of heating for the catastrophic-cooling loops heated below the transition region than for the non-catastrophic-cooling loops heated in the corona. We think that it is mainly due to the different conductive efficiency in these two regions. In the corona, the high conductive efficiency erases the effects of different manners of heating after the conductive cooling phase. However, the thermal conduction below the transition region is much less effective, so the effects of different heatings continue to the radiative cooling phase.

It should be pointed out that the length of the loop is a very important parameter to its evolution. As predicted by Mendoza-Briceño et al. (2005), the critical time for the loops from being long-lived to catastrophic cooling increases with the loop length. This is the reason why the inter-pulse time of 300 s in

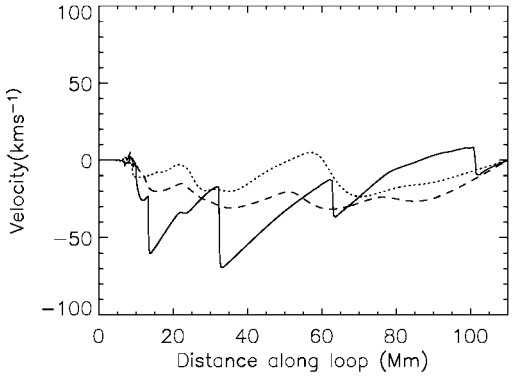

Fig. 9 Velocity profiles along the loop at $t = 5000$ s with heating located at $s_0 = 10$ Mm. Negative value means the downward velocities. Solid line, loop heated by a single pulse; dotted line, loop heated by five consecutive pulses; and dashed line, loop heated by five pulses with elapsed time of 300 s.

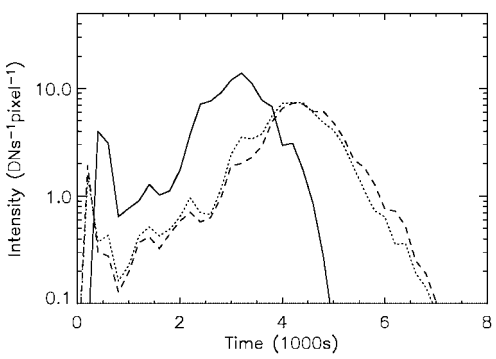

Fig. 10 Simulated intensity evolutions in TRACE 171 Å filter. Heating position is localized at $s_0 = 10$ Mm. Solid line, one pulse injected; dotted line, five pulses injected; and dashed line, ten pulses injected.

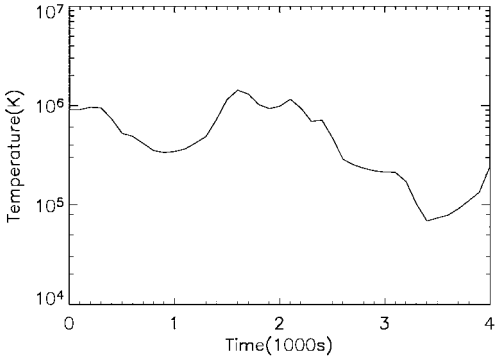

Fig. 11 Averaged temperature as a function of time. The loop is heated by five pulses with each pulse lasting 100 s. The first two pulses are injected in the initial 200 s, the rest three begin at $t = 1200$ s and end at $t = 1500$ s.

our study does not induce catastrophic cooling. We now set the elapsed time to a higher value and the result is shown in Figure 11. The catastrophic cooling now happens as predicted, though it does not take place in the heating phase as is presented in Mendoza-Briceño et al.(2005). The background heating increases the temperature from $t = 1000$ s during the long elapsed time from $t = 200$ s to $t = 1200$ s. This means not all the loops can experience catastrophic cooling during their heating stage by an increased inter-pulse time. Furthermore, the timescale for the loop to return to the equilibrium state depends on the total heating timescale. For the loops in Mendoza-Briceño et al.(2005), these two timescales are comparable; while for the loops in our work, the recovering timescales are much longer than the heating timescales. After the short-time heating terminates, the loops return to the elapsed time only by the background heating.

The exact properties of nanoflare heating are not well known till now. The assumptions about it in this paper are rather simple. More precise simulations should consider the energy distribution, exact energy value and the number of nanoflares, etc. In this paper the length of the loop is fixed at 110 Mm, we should consider as well other values because this parameter is also important to the loop evolution. These will be

investigated later. We think the instruments with higher quality, e.g., Solar B and STEREO, may further lead to much better insight in the research of coronal loop heating.

Acknowledgements We thank the referee for his comments and suggestions. We are grateful to Dr. Mariska for the guide on the code of SOLFTM (Solar Flux Tube Model) and Dr. Winebarger, Dr. Warren for some detailed help on the loop model calculated by SOLFTM. This work is supported by the National Natural Science Foundation of China through Grants 10333040 and 10221001, and by the Ministry of Science and Technology of China through Grant 2006CB806302.

References

Aschwanden M. J., 2004, Physics of the Solar Corona: An Introduction (Praxis Publishing Ltd., Chicester, UK)
Aschwanden M. J., Schrijver C. J., Alexander D., 2001a, ApJ, 550, 1036
Aschwanden M. J., 2001b, ApJ, 559, 171
Betta R., Reale F., Peres G., 1999, In: Proc. SOHO 8, Plasma Dynamics and Diagnostics in the Solar Transition Region and Corona, eds., J.-C. Vial, B. Kaldeich-Schümann, Noordwijk: ESA, p.179
Mariska J. T., 1987, ApJ, 319, 465
Mariska J. T., Emslie A. G., Li P., 1989, ApJ, 341, 1067
Mendoza-Briceño C. A., Erdélyi R., Sigalotti L. D. G., 2002, ApJ, 579, L49
Mendoza-Briceño C. A., Erdélyi R., 2004, In: Proc. SOHO 13, Waves, Oscillations and Small-Scale Transient Events in the Solar Atmosphere: A Joint View from SOHO and TRACE, ed. H. Lacoste, Noordwijk: ESA, p.261
Mendoza-Briceño C. A., Sigalotti L. D. G., Erdélyi R., 2005, ApJ, 624, 1080
Müller D. A. N., Peter H., Hansteen V. H., 2004, A&A, 424, 289
Parker E. N., 1988, ApJ, 330, 474
Priest E. R., Foley C. R., Heyvaerts J. et al., 2000, ApJ, 539, 1002
Reale F., Peres G, Serio S., 1994, In: IAU Colloq. 144, Solar Coronal Structures, eds. V. Rušin, P. Heinzel, Bratislava: Veda, 215
Reale F., Peres G., Betta R. M. et al. 2000, ApJ, 535, 423
Reale F., 2002, ApJ, 580, 566
Rosner R., Tucker W. H., Vaiana G. S., 1978, ApJ, 220, 643
Schrijver C. J., 2001, Sol. Phys., 198, 325
Testa P., Peres G., Reale F., 2005, ApJ, 622, 695
Warren H. P., Winebarger A. R., Mariska J. T., 2003, ApJ, 593, 1174
Winebarger A. R., Warren H. P., 2004, ApJ, 610, L129
Winebarger A. R., Warren H. P., Mariska J. T., 2003, ApJ, 587, 439